

STRUCTURAL INFLUENCE OF SERINE ON ZnO NANOSTRUCTURES

Shraddha Mahakal Assistant Professor, Department of Physics, Annasaheb Awate College, Manchar, Pune 410503, India.

Abstract:

A simple representative bio-composite, in which serine integrated ZnO nanostructures has synthesized by chemical method. In this study, the impact of serine on ZnO nanomaterial has been investigated in terms of structural, morphological, optical and bacterial properties. The X-ray diffraction of these bio-composites with pristine ZnO has indicated the induced strain in the ZnO matrix. The details of the structural study revealed modification in morphology of bio-composite along with variation in interplanar distance. The different properties of serine studies for different concentration in the surrounding climate of ZnO nanomaterial. It has been observed that serine has strong impression on ZnO as calculated strain increased from 1.11×10^{-3} to 3.28×10^{-3} . The morphology changes from hexagonal disc to hexagonal cross-sectional tubes grown in a particular direction with enhancement in visible luminescence compared to pristine ZnO. The biocompatibility of serine incorporated ZnO was noticed to enhance compared to ZnO in all the concentrations of serine.

Keywords: Nanomaterial, Serine, XRD, XPS & Bacterial properties.

Introduction:

A simple marriage of organic compound and inorganic semiconductor has now become energetic material owing to its dynamic properties and environmental point of view. The interface of these biomolecules with inorganic crystal has been a great significance in different aspects. There are many exquisite and fascinating examples of naturally occurring crystals, which are form in the environment of biomolecules. They are biologically controlled and adapted crystal system. Most of the properties of these materials are attributes to the presence of organic biomolecules such as at ntracrystalline and intercrystalline site of the crystal. The natural examples of the interaction of biomolecules with inorganic crystal are bone/teeth; configuration of DNA binding protein [1], mollusk seashell, zinc finger, guanine crystals found in the skin of many fish [2]. The interaction is keenly taking place in different way as per the type of amino acid and crystal. The proper selection of amino acid with particular concentration in synthetic crystal is the key factor for controlling its various properties.

ZnO is non-toxic, biosafe and biocompatible nanostructures. It is one of the special material with ample applications in optoelectronics [3], UV light emitters, transparent conducting electrode for solar cell flat panel display, UV lasers and sensors. ZnO is accessible in high quality bulk single crystal, with variety of morphologies. The requirement of simple synthesis technique and low cost with low temperature processing makes it unique material for employing it into device making. Thin films by doping of Mg in ZnO leads to change in band gap from 3.20 to 3.43eV whereas doping of Cd in ZnO changes band gap from 3.20 to 3.06 eV. ZnO is used in photo catalysis, varistor, and low-voltage phosphor materials.

Amino acids comprise of 1) Amine group 2) Carboxylic group and 3) Side chain group. These groups are making to amino acid to interact, incorporate, adsorb, adapt, modify, integrate, adhere and capping with inorganic crystal in a variety of way. The side chain of serine ($C_3H_7NO_3$) bears alcohol (-OH) group. Serine is non-essential amino acid for human being and has one of the simpler structures as compared to other amino acid. Many research groups have investigated the respond of amino acid on gold nanoparticles [4]. The carboxyl group in glutamine are active functional group for driving anisotropic growth for Ag nanoparticles [5,6]. The detail study of various amino acid interaction with ZnO has been systematically analysed and band gap alteration has reported [7]. They have observed the linear relationship between strain induced with modification in band gap of ZnO. In the review of Limo et al [8] the interfacing between metal oxide and biomolecules and their applications has elaborated. ZnO quantum dots functionalized with amino acids are utilized for detection of proteinase activity [9]. The band gap of ZnO can be finely and accurately tailored by amino acid [10]. From zinc acetate Schiff base complex can be obtained which when heated then ZnO nanoparticles having 50 to 110 nm size [11]. ZnO synthesized by the solvo-thermal reaction of zinc acetate with lysine, arginine and cysteine proved as a non-enzymatic glucose biosensor [12]. It has been reported that ZnO nanotriangles with ~ 160 -400nm height and ~ 170 -420nm edge were synthesized by microwave irradiation method using arginine as a capping agent are investigated as a water pollutant agent under solar irradiation [13]. The amino acid in ZnO matrix favors the radiative recombination resulting into strong confinement effect and efficient chirality transfer from amino acid to inter-band excitations in ZnO ;which can be arised by increase in the band gap [14].

The behavior of inorganic compound with the environment of biomolecules is tedious due to complex nature of biomolecules. By taking motivation from nature; our approach is to create biocompatible composite material consisting of ZnO nanostructures modified by amino acid. Moreover, serine has employed in this work to tune the properties of nanostructures of ZnO.

Material & Methods:

a) To carry out this study, Sigma-Aldrich procured $Zn(NO_3)_2 \cdot 6H_2O$ with 99.9% purity, Serine powder having 99.9% purity and NH_4OH (28.0-30.0% NH_3 basis) were used.

b) Synthesis of serine integrated ZnO nanoparticles:

For typical synthesis of serine integrated ZnO nanoparticles the solution of 0.25M Zn (NO₃)₂ with pH 6 was prepared in distilled water simultaneously 0.025mg of serine powder mixed. In the prepared solution drop-wise 1ml of NH₄OH was added, which thereafter, turns the solution to appear as white in colour. The obtained white colour solution has kept for homogeneous mixing and heating using magnetic stirrer in a silicon oil bath at 95°C for 90 min. After stirring the mixed solution allowed to cool naturally. The obtained white precipitates was then collected and centrifuge at 10,000 rpm of speed for 15 min and the washed repeatedly by distilled water and ethanol. Finally, the washed precipitate was dried at 140°C in a vacuum oven. The collected powder was treated as serine-integrated ZnO and referred as ZnO-S1 and further used for the characterization. In parallel to this we have synthesized other samples by taking serine powder in the concentration of 0.05, 0.075 and 1.0 mg and treated them as ZnO-S2, ZnO-S3 and ZnO-S4 respectively. Similarly, the above-mentioned synthesized powder without serine was referred as pristine ZnO.

Microtitre Plate Assay:

For the evaluation of antibacterial activity of the pristine ZnO and serine integrated ZnO, we have used microtiter-plate assay on *Escherichia coli* (*E. coli*) NCIM 2065 bacteria. These bacteria were obtained from the National Collection of Industrial Microorganisms (NCIM), National Chemical Laboratory (NCL), Pune, Maharashtra, India. The fresh culture was grown and maintained in nutrient broth (NB) (Himedia) at 37°C under shaking conditions (150 rpm). The stock solutions of synthesized powder samples were prepared with a concentration of 200 µg/ml in sterile distilled water. These solutions were then subjected to ultrasonicated for mixing of powders with water. Round bottomed 96 well microtiter polystyrene plates (Tarson, India) were used for this experiment.

Initially for the preparation of 96 well plates first row was assigned to serine, second assigned to ZnO, third assigned to ZnO-S1, fourth assigned to ZnO-S2, fifth assigned to ZnO-S3 and sixth assigned to ZnO-S4. Then 100 µl solution of sterile distilled water was added in column 2 to 12 wells. Now 200 µl of ZnO stock solution was added in second row of first column and then this solution is serially diluted till column 10 of first row by picking up 100 solution every time. The successive two fold dilution obtained were 100, 50, 25, 12.5, 6.25 and 3.12 µg/ml. Same steps were repeated for ZnO-S1, ZnO-S2, ZnO-S3 and ZnO-S4. For the standard negative control reading 50 µl of sterile MHB solution was added in 11th well. Now 50 µl of McFarland adjusted culture was added in well of 1 to 10. For the standard positive control reading 50 µl McFarland adjusted culture was added in 12th well.

The above-mentioned preparation of 96 well plates was done in three sets. These prepared three sets of plates were incubated overnight at 37°C and ELISA microtiter plate reader (Spectramax M2, USA) was used to measure the optical density (OD) at wavelength = 540 nm. The growth inhibition percentages of *E. coli* at different concentrations were calculated using following relation

$$\text{Percentage cell inhibition} = \frac{(A_t - A_b)}{(A_c - A_b)} \times 100$$

where, A_t is OD of test compound, A_b is OD of blank (negative control) and A_c is a OD of control (positive control).

Characterization:

The structural analyses of the samples were taken by X-Ray Diffraction (XRD). It was performed using Bruker AXS D8 Advance Diffractometer. FESEM images for control of *E. coli* cells were captured by FEI-SEM, QUANTA 200 3D, tungsten filament. SEM pictures were taken by JEOL, JSM-6360A. The microtiter plate reading were recorded by microtiter plate reader SpectraMax M2.

Result & Discussion:**X-Ray Diffraction:**

XRD is first step for the analysis of structure, phase and crystallinity of the serine modified ZnO nanoparticles. Following figure 1 indicates the XRD pattern of synthesized ZnO nanoparticles and ZnO nanoparticles with increasing the concentration of serine in θ - 2θ scan mode. The diffraction pattern of ZnO shows pure and crystalline phase. Additional peaks corresponding to impurities like Zn, Zn-OH or Zn(OH)₂ are not observed in ZnO control sample. All the diffraction prominent peaks are corresponding to Wurtzite structure having JCPDS Card No. 01-079-2205 with space group P63mc. The increase in concentration of serine in ZnO host has not altered the crystal structure for ZnO-S1 and ZnO-S2. Whereas a new peak is observed at $\sim 57^\circ$ (labeled by *) for ZnO-S3 and ZnO-S4 concentration. For higher concentration of serine (0.15 mg/mL) the series of additional peaks were observed. The Bragg's diffraction peaks of serine modified ZnO manifest little reposition. The diffraction peaks are shifted and broadening is seen which are the implications of change in lattice parameters due to intervening of serine molecule with the ZnO.

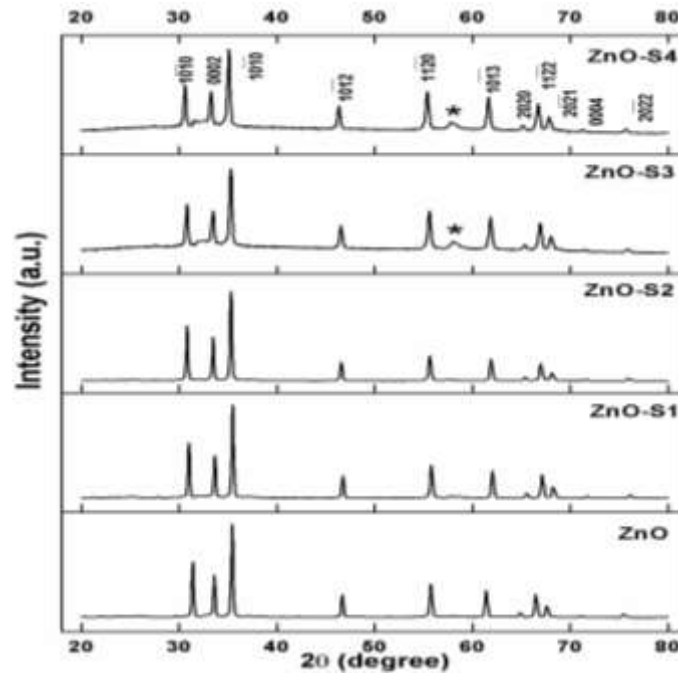
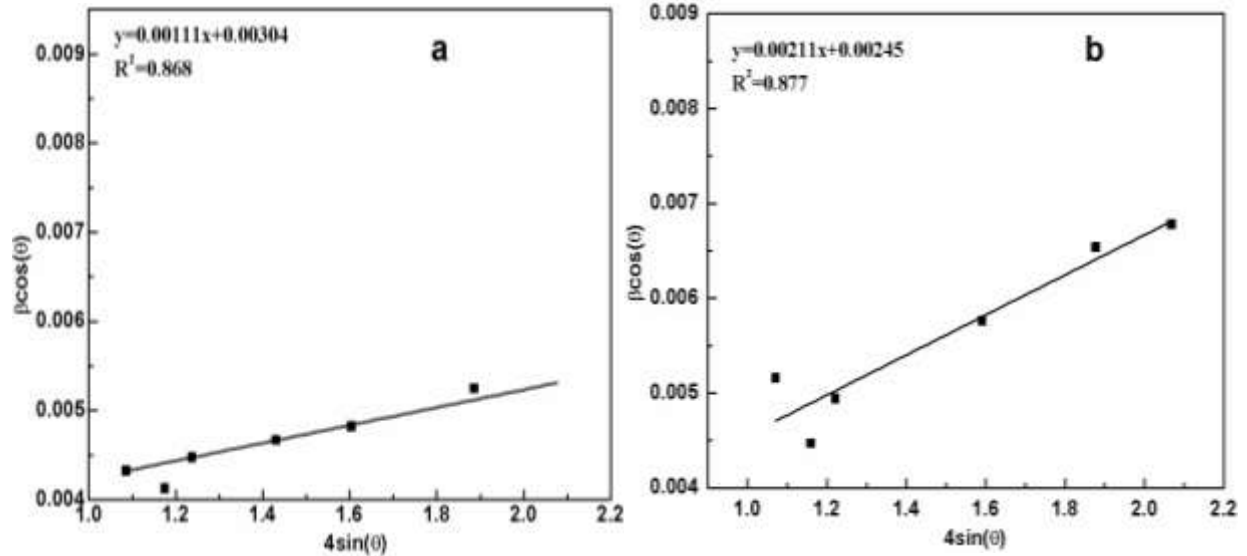


Figure 1 XRD pattern for ZnO and serine modified ZnO

Table 1 Variation of FWHM for the 10 $\bar{1}$ 0 and 0002 planes by incorporation of Serine

Sample	FWHM(degree)		d-spacing (Å^0)	
	10 $\bar{1}$ 0	0002	10 $\bar{1}$ 0	0002
ZnO	0.192	0.158	2.8464	2.6645
ZnO-S1	0.200	0.202	2.8826	2.6680
ZnO-S2	0.216	0.202	2.9010	2.6788
ZnO-S3	0.221	0.214	2.9010	2.6788
ZnO-S4	0.255	0.221	2.9197	2.6940



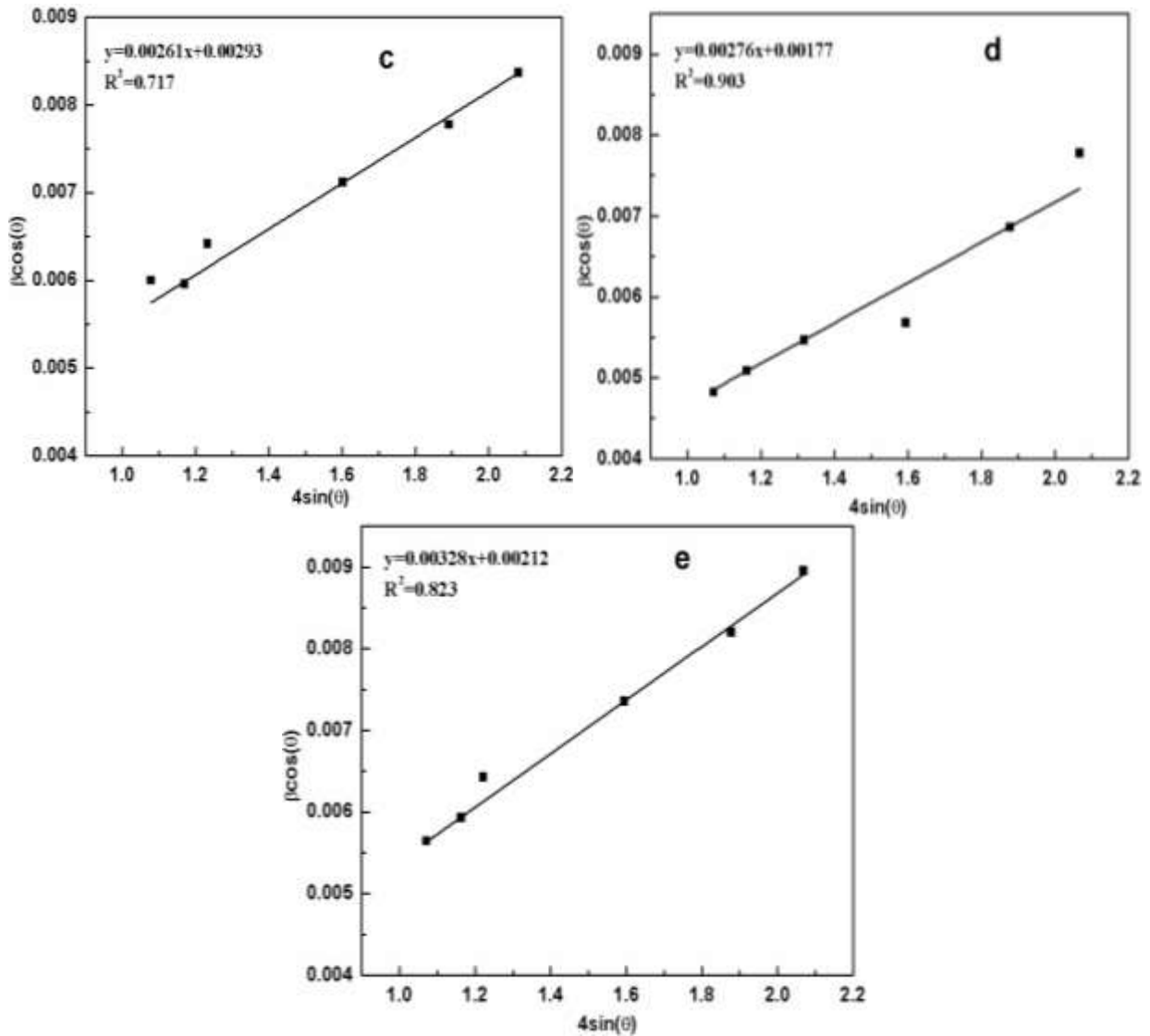


Figure 2 Strain estimation from W.H. method for :a) ZnO , b)ZnO-S1, c)ZnO-S2 ,d)ZnO-S3 and e) ZnO-S4nanoparticles

Table 2 Representation of strain and size with serine estimated by W.H.method

Sample	$\epsilon(X10^{-3})$	D (nm)
ZnO	1.11	30.4
ZnO-S1	2.11	24.5
ZnO-S2	2.61	29.3
ZnO-S3	2.76	17.7
ZnO-S4	3.28	21.2

The diffraction peaks revealed slight shift towards lower angle for the ZnO-S3 and ZO-S4 samples. The lattice parameters calculated for ZnO and serine mediated ZnO shows the intervening of serine in ZnO leads to develop strain in the crystal. The c-axis has observed to strained maximum as compared to other lattice parameters due to incorporation. Since, serine has shown different communication with different faces of ZnO as both lattice parameters are showing different strain by addition of serine. In addition, with this the intervening of serine leads to width of the diffraction peaks to increase. The observed FWHM of peak is consequence of sample and instrument. Therefore, for accurate calculation of size and strain the FWHM was corrected by following equation (I) given by

$$\beta = [(\beta_M)^2 - (\beta_s)^2]^{1/2} \text{-----(I)}$$

where, β_M is measured FWHM and β_s is instrumental FWHM. The FWHM corrected by above formula corresponding to peaks $10\bar{1}0$ and 0002 are indicated in following table 1. Eventually the average crystallite size also decreases with serine. The average crystallite size calculated by modified Scherrer formula given by

$$\text{average crystallite size} = \left(\frac{K\lambda}{\sqrt{(\beta_M^2 - \beta_S^2)} \cos\theta} \right) + \eta \tan\theta \text{ -----(II)}$$

where, K is the shape factor ~ 0.9 , β_M is the measured FWHM of the diffraction peak where the Bragg's condition is satisfied and β_S is instrument FWHM from the standard sample, η is the strain observed along c -axis. The influence of various amino acid on calcite was screened and calcite crystal responds to amino acid by generation of lattice strain and distortion [15]. The average crystallite size found to be ~ 31 nm.

It is evident from above table that serine incorporation generates impact on particle size, lattice parameter and interplanar distance. In another words serine induces the lattice distortion in ZnO host crystal. The concentration for ZnO-S4 shows maximum influence on ZnO matrix.

Generally, strain induced in lattice parameter and sizes are responsible for peak broadening. The strain developed can be given by $\epsilon \approx \beta/4\tan\theta$. We have employed Williamson-Hall method for the details of strain induced by serine in ZnO matrix. The Williamsons-Hall equation in uniform deformation model is given by

$$\beta \cos\theta = \frac{K\lambda}{D} + 4\epsilon \sin\theta \text{ -----(III)}$$

where, K is the shape factor ~ 0.9 , D is crystallite size, ϵ is strain developed due to crystal imperfection and distortion. Above equation III presumes the strain is uniform in all directions. The value of $\beta \cos\theta$ and $4\epsilon \sin\theta$, was taken from y -axis and x -axis respectively; linear fitting of this graph was done. The strain was calculated from the slope and crystallite size was estimated from y -intercept of the linear fitted line. The observed strain and size of the samples with increase in serine concentration is given in the table 2.

Room Temperature Photoluminescence:

The important characteristics of optical properties of the composite can analyzed by photoluminescence study. This technique investigates band gap and defect of impurity induced transitions. Fig. 3 displays the room temperature photoluminescence of ZnO and ZnO-Si ($i=1-4$) composite within the wavelength of 350-600nm. All samples indicate intense and broad peak at ~ 376.77 nm in agreement with the earlier reported data [16]. This peak is observed due to significant absorption at absorption edge of ZnO. Xiao et al. has been analyzed broadening and splitting in near band edge in UV region in case of 20nm grain and also had discussed that this observation of broadening can assigned to quantum confinement effect [17].

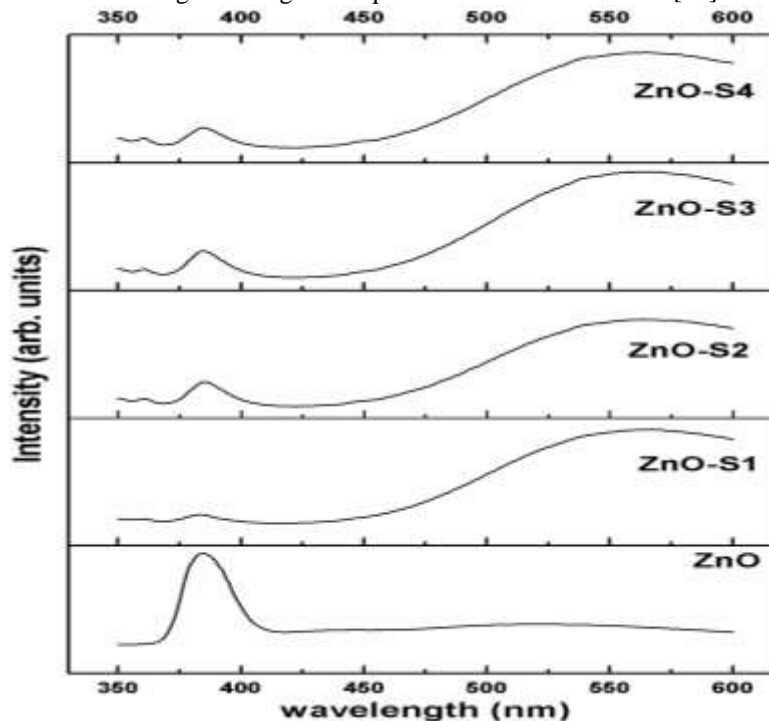


Figure 3 Room Temperature Photoluminescence of ZnO with increase in serine

Accompanying with this all synthesized samples exhibits broad luminescence band between the wavelength scale of ~ 450 - 600 nm was observed. Since this broad luminescence is less prominent in ZnO while it becomes more intense in the serine-ZnO composite with serine. It was reported that the inception of violet is presence of zinc interstitial [18], zinc vacancy [19]. Blue emissions are observed due to oxygen vacancy [20]. This broad luminescence band observed in the visible region has cardinal importance in determining the defects present in ZnO samples. Impurity atoms are also responsible for this contribution in visible

scale. Intrinsically in ZnO lattice zinc atoms are located at half of tetrahedral positions and octahedral sites are empty [21]. This leads to availability of favorable condition of atoms to accommodate and defects are inherently present. Serine ($C_3H_7NO_3$) integration in ZnO matrix has generated more intense visible luminescence as compared to ZnO which implies that the defects are enhanced due to serine.

SEM:

Morphological analysis of the synthesized samples is effectively done by FE-SEM. Serine mediated ZnO nanostructure was synthesized at pH 8-9 in this study. Serine is either protonated or deprotonated decided by pH of the solution. Serine has pKa value 2.21 for terminal carboxyl group and 9.15 for terminal α -amino group. It has CH_2OH as a side chain. At pH 8-9 carboxyl group is deprotonated ($pH > pK_a$ of $-CO_2H$) whereas amino group is half protonated and half deprotonated (as little difference between pH & pKa of $-NH_3^+$). Along these lines the overall charge on serine molecule is -0.5 by carboxylic acid at pH ~9. Thus owing to the interaction between serine and ZnO the morphology get altered. The transition in morphology has revealed by the SEM images shown in figure 4.

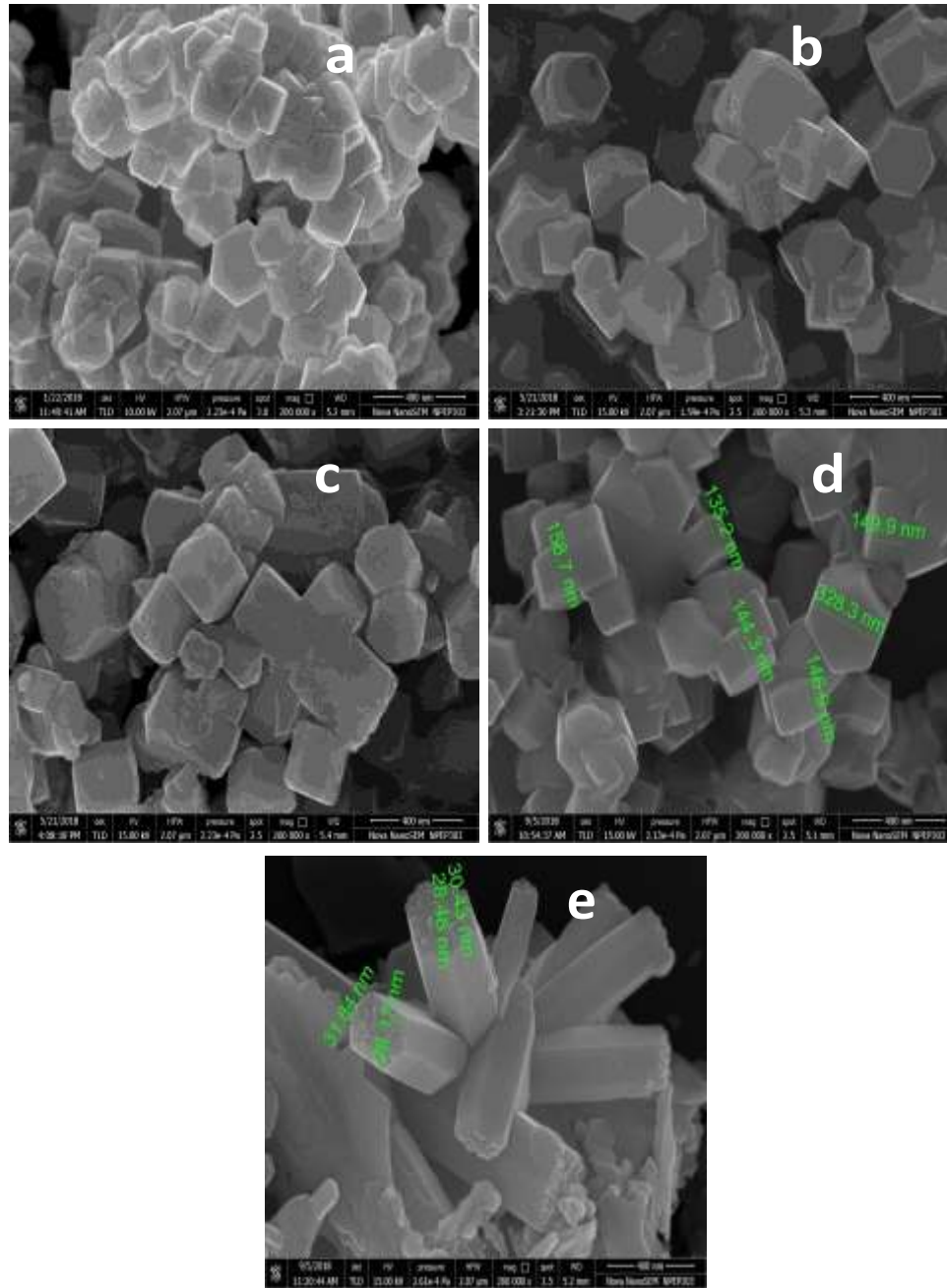


Figure 4 FE-SEM images of synthesized samples with increase in serine concentration: a) ZnO, b) ZnO-S1, c) ZnO-S2, d) ZnO-S3 and e) ZnO-S4

SEM image of ZnO has depicted the hexagonal disc like structure which is greatly varied as serine intervening takes place. The crystal growth gets favored in a particular direction as directed by serine molecules. Preferentially COO⁻ group reacts with ZnO surface which results to advance in morphology [22]. The crystallite size estimated by W.H. method agrees with the size observed by FE-SEM images.

X-Ray Photoelectron Spectroscopy (XPS):

The sample was taken in the palletized form for the XPS spectra. For the identification of existence of serine in the synthesized samples we have performed the XPS. The analysis of the XPS spectra of carbon atom was performed. The fig. 5 represents the XPS of Carbon atom in the serine modified sample of ZnO for maximum concentration of serine (ZnO-S4). It exhibits the sign of confirmation of serine molecules communication with ZnO. The deconvoluted peak of C1S shows three distinct peaks. First peak observed at 284.89eV which attributes to carbon atom belonging to methyl group, 286.65eV corresponding to carbon atom belonging to carbon atom in the environment of Nitrogen atom of amino group and 288.70eV attributed to carbon atom belonging to carboxyl group. The same species were observed in the interaction of alanine with ZnO surface [22]. Only single peak corresponding to carbon atom was observed in the pristine ZnO sample.

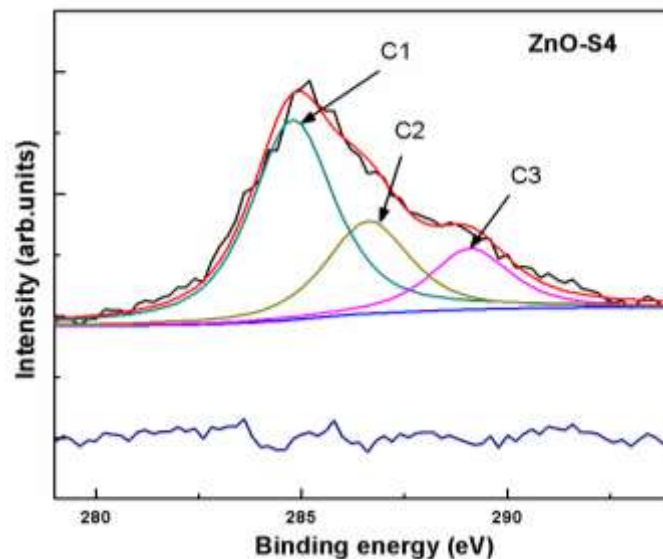


Figure5. XPS of C1S peak with maximum concentration of serine in ZnO

Microtitre Plate Assay:

To evaluate the effect of serine on antibacterial activity of ZnO we have performed this assay for *E.coli* we have used above mentioned equation 3). Figure 6 shows the divergence in percentages of cells inhibited with varying concentrations of ZnO and serine integrated composite. It is evident that ZnO shows good antibacterial activity as expected whereas the composite shows decreasing in it as serine concentration increases. This is revealed that the % cell inhibition of *E.coli* in the presence of the synthesized samples is indicating unprecedented observation as compared with pristine ZnO.

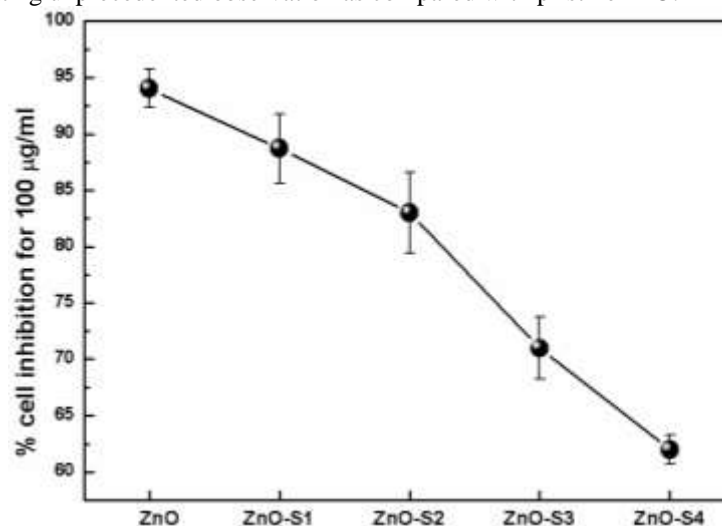


Figure6 % cell inhibition of *E.coli* by the samples

Conclusion: Current study concludes that the biomolecules like amino acid are playing crucial role with the interaction of inorganic material. While in composite of serine with ZnO the crystal structure indicates development of strain in the ZnO crystal, remarkable modification in morphology and enhancement in visible luminescence. The XPS spectra of carbon atom show footprints of existence of serine in the synthesized composite. The integration of serine in ZnO has confirmed by weaning of antibacterial activity of ZnO. This trend of weaning of antibacterial activity of ZnO has observed with increase in concentration of serine.

Acknowledgement: Authors are thankful to Savitribai Phule Pune University, Pune for providing lab facility to carry out this study. S.Mahakal specially thanks to UGC and Annasaheb Awate College, Manchar for providing support under scheme.

Reference:

- [1] Lippard, S.J. and Berg, J.M., 1994. *Principles of bioinorganic chemistry* (Vol. 70). Mill Valley, CA: University Science Books.
- [2] Levy-Lior, A., Shimoni, E., Schwartz, O., Gavish-Regev, E., Oron, D., Oxford, G., Weiner, S. and Addadi, L., 2010. Guanine-based biogenic photonic-crystal arrays in fish and spiders. *Advanced Functional Materials*, 20(2), pp.320-329.
- [3] Djurišić, A.B., Ng, A.M.C. and Chen, X.Y., 2010. ZnO nanostructures for optoelectronics: Material properties and device applications. *Progress in quantum electronics*, 34(4), pp.191-259.
- [4] Bhargava, S.K., Booth, J.M., Agrawal, S., Coloe, P. and Kar, G., 2005. Gold nanoparticle formation during bromoaurate reduction by amino acids. *Langmuir*, 21(13), pp.5949-5956.
- [5] Xie, J., Lee, J.Y., Wang, D.I. and Ting, Y.P., 2007. Silver nanoplates: from biological to biomimetic synthesis. *ACS nano*, 1(5), pp.429-439.
- [6] Dickerson, M.B., Sandhage, K.H. and Naik, R.R., 2008. Protein- and peptide-directed syntheses of inorganic materials. *Chemical reviews*, 108(11), pp.4935-4978.
- [7] Brif, A., Ankonina, G., Drathen, C. and Pokroy, B., 2014. Bio-Inspired Band Gap Engineering of Zinc Oxide by Intracrystalline Incorporation of Amino Acids. *Advanced Materials*, 26(3), pp.477-481.
- [8] Limo, M.J., Sola-Rabada, A., Boix, E., Thota, V., Westcott, Z.C., Puddu, V. and Perry, C.C., 2018. Interactions between metal oxides and biomolecules: from fundamental understanding to applications. *Chemical reviews*, 118(22), pp.11118-11193.
- [9] Popow-Stellmaszyk, J., Bajorowicz, B., Malankowska, A., Wysocka, M., Klimczuk, T., Zaleska-Medynska, A. and Lesner, A., 2018. Design, synthesis, and enzymatic evaluation of novel ZnO quantum dot-based assay for detection of proteinase 3 activity. *Bioconjugate chemistry*, 29(5), pp.1576-1583.
- [10] Pokroy, B. and Anastasia, B.R.I.F., Technion Research and Development Foundation Ltd, 2017. *Crystals of semiconductor material having a tuned band gap energy and method for preparation thereof*. U.S. Patent 9,771,263.
- [11] Gharagozlou, M., Baradaran, Z. and Bayati, R., 2015. A green chemical method for synthesis of ZnO nanoparticles from solid-state decomposition of Schiff-bases derived from amino acid alanine complexes. *Ceramics International*, 41(7), pp.8382-8387.
- [12] Tarlani, A., Fallah, M., Lotfi, B., Khazraei, A., Golsanamlou, S., Muzart, J. and Mirza-Aghayan, M., 2015. New ZnO nanostructures as non-enzymatic glucose biosensors. *Biosensors and Bioelectronics*, 67, pp.601-607.
- [13] Bhattacharjee, A. and Ahmaruzzaman, M., 2018. α -Amino acid assisted facile synthesis of two-dimensional ZnO nanotriangles for removal of noxious pollutants from water phase. *Journal of environmental chemical engineering*, 6(4), pp.4970-4979.
- [14] Muhammed, M.A.H., Lamers, M., Baumann, V., Dey, P., Blanch, A.J., Polishchuk, I., Kong, X.T., Levy, D., Urban, A.S., Govorov, A.O. and Pokroy, B., 2018. Strong Quantum Confinement Effects and Chiral Excitons in Bio-Inspired ZnO–Amino Acid Cocrystals. *The Journal of Physical Chemistry C*, 122(11), pp.6348-6356.
- [15] Borukhin, S., Bloch, L., Radlauer, T., Hill, A.H., Fitch, A.N. and Pokroy, B., 2012. Screening the incorporation of amino acids into an inorganic crystalline host: the case of calcite. *Advanced Functional Materials*, 22(20), pp.4216-4224.
- [16] Kunj, S. and Sreenivas, K., 2016. Residual stress and defect content in magnetron sputtered ZnO films grown on unheated glass substrates. *Current Applied Physics*, 16(7), pp.748-756.
- [17] Xiao, S.S., Zhao, L., Liu, Y.H. and Lian, J.S., 2013. Nanocrystalline ZnO films prepared by pulsed laser deposition and their abnormal optical properties. *Applied surface science*, 283, pp.781-787.
- [18] Yang, Q., Tang, K., Zuo, J. and Qian, Y., 2004. Synthesis and luminescent property of single-crystal ZnO nanobelts by a simple low temperature evaporation route. *Applied Physics A*, 79(8), pp.1847-1851.
- [19] Heo, Y.W., Norton, D.P. and Pearton, S.J., 2005. Origin of green luminescence in ZnO thin film grown by molecular-beam epitaxy. *Journal of Applied Physics*, 98(7), p.073502.
- [20] Chia, M.Y., Chiu, W.S., Daud, S.N.H., Khiew, P.S., Radiman, S., Abd-Shukor, R. and Hamid, M.A.A., 2015. Structural- and optical-property characterization of three-dimensional branched ZnO nanospikes. *Materials Characterization*, 106, pp.185-194.
- [21] Schmidt-Mende, L. and MacManus-Driscoll, J.L., 2007. ZnO–nanostructures, defects, and devices. *Materials today*, 10(5), pp.40-48.
- [22] Gao, Y.K., Traeger, F., Shekhah, O., Idriss, H. and Wöll, C., 2009. Probing the interaction of the amino acid alanine with the surface of ZnO (101⁻0). *Journal of colloid and interface science*, 338(1), pp.16-21.